



# Asymmetric synthesis of (*S*)-ethyl-4-chloro-3-hydroxy butanoate using a *Saccharomyces cerevisiae* reductase: Enantioselectivity and enzyme–substrate docking studies

Jihye Jung<sup>a</sup>, Hyun Joo Park<sup>a</sup>, Ki-Nam Uhm<sup>b</sup>, Dooil Kim<sup>c</sup>, Hyung-Kwoun Kim<sup>a,\*</sup>

<sup>a</sup> Division of Biotechnology, The Catholic University of Korea, Bucheon 420-743, Republic of Korea

<sup>b</sup> Equispharm Ltd., Daejeon 305-811, Republic of Korea

<sup>c</sup> Systems Microbiology Research Center, Korea Research Institute of Bioscience and Biotechnology, Daejeon 305-806, Republic of Korea

## ARTICLE INFO

### Article history:

Received 2 February 2010

Received in revised form 5 June 2010

Accepted 14 June 2010

Available online 20 June 2010

### Keywords:

Reductase

Enantioselectivity

Chiral intermediate

Hyperlipidemia drug

Docking model

## ABSTRACT

Ethyl (*S*)-4-chloro-3-hydroxy butanoate (ECHB) is a building block for the synthesis of hypercholesterolemia drugs. In this study, various microbial reductases have been cloned and expressed in *Escherichia coli*. Their reductase activities toward ethyl-4-chloro oxobutanoate (ECOB) have been assayed. Among them, Baker's yeast YDL124W, YOR120W, and YOL151W reductases showed high activities. YDL124W produced (*S*)-ECHB exclusively, whereas YOR120W and YOL151W made (*R*)-form alcohol. The homology models and docking models with ECOB and NADPH elucidated their substrate specificities and enantioselectivities. A glucose dehydrogenase-coupling reaction was used as NADPH recycling system to perform continuously the reduction reaction. Recombinant *E. coli* cell co-expressing YDL124W and *Bacillus subtilis* glucose dehydrogenase produced (*S*)-ECHB exclusively.

© 2010 Elsevier B.V. All rights reserved.

## 1. Introduction

The asymmetric reduction of ketones to optically pure alcohols has become the focus of a great deal of attention, primarily in regard to their possible use as chemotherapeutic drugs and chiral building blocks. Many oxidoreductase enzymes from a variety of microorganisms are capable of reducing carbonyl groups with chemo-, regio-, and stereoselectivity [1,2].

Enzymatic ketone reductions can be achieved via the use of either isolated enzymes [1,3,4] or whole cell systems [5–7]. The use of isolated enzymes is advantageous in that undesirable enantiomer formation mediated by contaminating ketoreductases is minimized, and the enzymes can be stored and employed as normal chemical reagents. On the other hand, whole cell biocatalysts are more stable, due to the protective effects of the cell membrane. Enzyme purification is unnecessary when whole cells are applied as biocatalysts. Additionally, the reductase reaction can be performed using endogenous NAD(P)H as a cofactor, even without the addition of external NAD(P)H. If recombinant *Escherichia coli* cells co-expressing both a specific reductase and glucose dehydrogenase (GDH) are used, not only is undesirable enantiomer formation minimized, but the continuous recycling of NAD(P)H is also enabled [5,6,8].

Kamitori et al. previously elucidated the X-ray crystal structures of *Sporobolomyces salmonicolor* carbonyl reductase and its complex with NADPH (PDB ID 1Y1P) [9]. They were the first to propose the hydrogen bonding residues that fix the carbonyl oxygen of substrates in the active site and hydrophobic channel. Hua et al. conducted a molecular modeling analysis of different aryl alkyl ketones in the 1Y1P active site in order to gain insight into the enantioselectivity observed in the aryl alkyl ketone reduction [10].

In a previous study, we generated 10 different microbial reductases [11]. In this work, we screened 3 enzymes among them, which were capable of generating each enantiomer of ethyl 4-chloro-3-hydroxy butanoate (ECHB), a chiral intermediate in hyperlipidemia drugs. According to the results of the product analysis and the protein structure modeling study, YDL124W was finally selected for the production of (*S*)-ECHB. The properties of the selected carbonyl reductase were characterized and recombinant *E. coli* cells performing the reductase-glucose dehydrogenase-coupling reaction were constructed in order to generate (*S*)-ECHB efficiently.

## 2. Materials and methods

### 2.1. Chemicals

Ethyl-4-chloro-3-oxo butanoate (ECOB), glucose dehydrogenase (GDH, *Thermoplasma acidophilum*), NAD(P)H, and NAD(P)<sup>+</sup> were purchased from Sigma-Aldrich Co. (St. Louis, MO). (*R*)- and (*S*)-ethyl-

Abbreviations: ECOB, ethyl-4-chloro-3-oxo butanoate; ECHB, ethyl-4-chloro-3-hydroxy butanoate; GDH, glucose dehydrogenase; NAD(P)H, nicotinamide adenine dinucleotide (phosphate); DMSO, dimethyl sulfoxide; GC, gas chromatography

\* Corresponding author. Tel.: +82 2 2164 4890; fax: +82 2 2164 4865.

E-mail address: [hkkim@catholic.ac.kr](mailto:hkkim@catholic.ac.kr) (H.-K. Kim).

4-chloro-3-hydroxy butanoate ((*R*)- and (*S*)-ECHB) were received from Equispharm Ltd. (Korea). All other chemicals were of analytical grade.

### 2.2. Reductase and glucose dehydrogenase activity assay

Reductase activity was evaluated at 30 °C by measuring the reduction in absorbance at 340 nm for 5–10 min using a spectrophotometer. The reaction mixture (1 mL) consisted of 1 mM ECOB (100 mM stock in DMSO), 0.2 mM NAD(P)H, 50 mM potassium phosphate (pH 6.5) buffer, and 5–50  $\mu$ L of cell-free extract or 10  $\mu$ L of the permeabilized cells. One unit of enzyme was defined as the quantity of enzyme required to catalyze the oxidation of 1  $\mu$ mol NAD(P)H in 1 min at 30 °C.

The oxidation reaction mixture (1 mL) of glucose dehydrogenase consisted of 10 mM glucose, 0.2 mM NADP<sup>+</sup>, 50 mM potassium phosphate (pH 6.5) buffer, and 0.1  $\mu$ L of commercial glucose dehydrogenase or 10  $\mu$ L of the permeabilized cells. The reaction rate was monitored using a spectrophotometer on the basis of the increase in absorbance at 340 nm for 5–10 min at 30 °C. One unit of enzyme was defined as the quantity required to reduce 1  $\mu$ mol of NADP<sup>+</sup> in 1 min at 30 °C.

### 2.3. Computational methods

The 3D model structure of YOL151W was determined in previous studies [11]. In this research, the initial 3D model structures of YDL124W and YOR120W from *Sacharomyces cerevisiae* were constructed on the basis of the crystal structures of two aldo-keto reductases (PDB code: 3BUV [12] and 1C9W [13], respectively). The identity of the entire amino acid sequences of YDL124W and 3BUV was calculated to be 30.7% by ClustalW method in DNASTAR program. The identity of YOR120W and 1C9W was calculated to be 39.4% by the same method.

The target structures were modeled *in silico* via a structural homology search using HHpred/HHsearch [14,15] and homology modeling using MODELLER [16], then optimized using FoldX [17]. The active sites of YDL124W and YOR120W were evaluated via comparison with two corresponding X-ray templates. The geometries of the substrate (ECOB) and cofactor (NADPH) were optimized using the Hartree-Fock method with a 6-31G\* basis set as implemented in the Gaussian 03 program (Gaussian, Inc., Wallingford, CT). The restrained electrostatic potential procedure of the Antechamber module from the AMBER suite was used to generate input files with charges for docking programs [18,19]. The results were then utilized as valid inputs for the AutoDock ligand preparation procedure.

Docking was conducted with AutoDock (ver. 4.0), using the implemented empirical free energy function and the Lamarckian genetic algorithm [20]. The best docked conformations were those determined to have the lowest binding energy and the greatest number of members in the cluster, thereby indicating good convergence. The best orientation was identified and optimized using the scoring function based on the AMBER force field FF99 and energy minimization according to the Nelder and Mead algorithm [19] for induced-fit simulation. The parameters embedded in the AMBER package were used for energy minimization and molecular dynamics [21,22]. Molecular dynamics (MD) simulations were also conducted. Additionally, the docking of ECOB and NADPH to our target proteins was initially assessed in accordance with the topological binding sites predicted by several algorithms [23].

Structurally variable region (loop, Ile120-Lys127) was generated by sampling main-chain dihedral angles built randomly using the discrete optimized protein energy (DOPE)-based loop modeling protocol in MODELLER software. Each loop takes the initial conformation and randomizes it by  $\pm 3$  Å in each of the Cartesian coordinates. Thousand loop structures for Ile120-Lys127 were ranked on the basis

of their energy (DOPE) and cubic spline restraints integrated in MODELLER. The side chains were then modeled while avoiding steric clashes, but also keeping the existing other side chains automatically. The model structure is then optimized by the method of conjugate gradients combined with molecular dynamics and simulated annealing [24]. This method was used to relieve steric clashes and overlaps of side chains. The loop refinement relies on an atomistic distance-dependent statistical potential of mean force for non-bond interaction [25]. The stereochemical properties of minimized structures were evaluated by Ramachandran plot calculations computed with Procheck program [26]. Profile-3D [27,28] further confirms the environment of side chains and examines the misfolded regions. RMSD fit was calculated by alignment of structural homology feature in MODELLER.

### 2.4. Purification of reductase YDL124W

Reductase YDL124W was identified as an appropriate enzyme for the reduction of ECOB to (*S*)-ECHB in an enantioselective fashion. The reductase protein in the cell-free extract was purified as follows. First, the cell-free extract was loaded onto a Ni-NTA column (QIAGEN GmbH, Hilden) equilibrated with a 50 mM Tris-HCl buffer (pH 7.8) containing 50 mM imidazole and 300 mM NaCl. After washing with the same buffer, the YDL124W was eluted from the column via the application of a 200 mM imidazole buffer. The active fractions were then collected and desalted with a PD-10 desalting column (GE Healthcare Bio-Sciences AB, UK).

### 2.5. Effect of temperature and pH

The effects of temperature and pH were evaluated using the purified YDL124W enzyme. Reactions were monitored spectrophotometrically by measuring the reduction in NADPH at 340 nm with the purified enzyme. The reaction rate was measured at various temperatures (5–60 °C). Meanwhile, in order to evaluate temperature stability, the enzyme was pre-incubated for 30 min at 10–45 °C, after which the remaining activity was assayed at 30 °C. The following buffers (50 mM) were utilized to assess the effects of pH: pH 3–6.5, acetic acid/sodium acetate; pH 6.5–8, KH<sub>2</sub>PO<sub>4</sub>/K<sub>2</sub>HPO<sub>4</sub>; pH 7.5–9, Tris-HCl; pH 9–10.5, glycine-KCl-KOH. To confirm the pH stability, the enzyme was pre-incubated in the pH buffers listed above for 30 min on ice, then adjusted to pH 6.5, under which conditions the enzyme's residual activity was evaluated.

### 2.6. Effect of concentration of buffer and DMSO

The effect of the potassium phosphate buffer concentration on the reductase reaction rate was measured. Various concentrations (50, 100, 150, 200, 250, 300 mM) of potassium phosphate buffer (pH 6.5), including 1 mM ECOB, 0.2 mM NADPH and 5  $\mu$ L of purified enzyme were used.

Reaction solutions (50 mM potassium phosphate buffer, pH 6.5) containing 1 mM ECOB, 0.2 mM NADPH, 5  $\mu$ L of purified enzyme, and various concentrations of DMSO (final conc. 1, 3, 10, 15, 20, and 30%, v/v) were mixed, and the reaction rates were measured by determining the decrease in absorbance at 340 nm.

### 2.7. Enzymatic coupling reaction and reaction mixture analysis

The enantioselectivity of the enzymatic reduction of ECOB was evaluated. The general procedure was as follows: 100 mM ECOB, 1 mM NADPH, 13 units of reductase YDL124W, 150 mM D-glucose, and 26 units of commercial glucose dehydrogenase were mixed in a total volume of 15 mL of potassium phosphate buffer (50 mM, pH 6.5), and the mixture was incubated at 25 °C. The pH of the reaction mixture was monitored with a pH meter and maintained at 6.0–6.5 via the addition of 1 M NaOH.

For the coupling reactions using the whole cell systems, 100 mM ECOB, 1 mM NADPH, 150 mM D-glucose, and 13 units (reductase activity) of the permeabilized cells containing two plasmids (pETR124 and pACGDH) or one plasmid (pACR124-GDH), were mixed in a total volume of 15 mL of potassium phosphate buffer (50 mM, pH 6.5), and the mixture was incubated at 25 °C.

Aliquots (100 µL) of the reaction mixture were sampled, mixed with 400 µL of ethyl acetate and 50 µL of saturated K<sub>2</sub>CO<sub>3</sub>, then centrifuged for 10 min at 10000×g. The ethyl acetate (250 µL) layer was obtained, dried via speedvac, dissolved with methylene chloride (400 µL), and mixed with 20 µL of pyridine and 10 µL of acetyl chloride. After 1 h of incubation, the mixture was washed with 1 M HCl (200 µL) and saturated NaHCO<sub>3</sub> (200 µL). The organic phase was then analyzed using a GC system equipped with a chirasil-dex column (Varian LTD.). The column temperature was increased from 70 °C to 180 °C at a rate of 5 °C per min and maintained for 2 min at 180 °C. A flame ionization detector was used to analyze the quantity of alcohols generated by enzymatic reduction. By comparing the retention times and peak areas of standard (*R*)- and (*S*)-alcohol peaks, the total quantities (in moles) of products in the reaction mixtures were calculated.

### 2.8. Co-expression of reductase and glucose dehydrogenase in *E. coli*

To obtain *Bacillus subtilis* glucose dehydrogenase, a PCR primer set was designed on the basis of the nucleotide sequence information in the NCBI GenBank database (EF626962.1) as follows: 5'-CGCCATATG-TATCCGGATTTAAAGGA-3'/5'-ATAGTACCTTAACCGCGGCTGCCTG-3'. The genomic DNA of *B. subtilis* was used as a template. The PCR conditions were as follows: 30 cycles of 95° C for 1 min, 43° C for 1 min and 72° C for 1 min. The PCR product was cloned into pGEM-T (Promega Corp., Madison, WI) and transformed into *E. coli* XL1-Blue. The *Bacillus* GDH gene in pGEM-T vector was cut with *Nde*I and *Kpn*I, then ligated downstream of the second T7 promoter of the pACYCDuet-1 vector and used to transform *E. coli* BL21 (DE3). The recombinant plasmid was designated as pACGDH.

A recombinant plasmid harboring both the YDL124W gene and the *Bacillus* GDH gene was also constructed as follows. In order to subclone the YDL124W reductase gene into pACGDH, the following PCR primer set was designed: 5'-GAGCCATGGCATCATTTACCAACAGTTC-3'/5'-GCCAAGCTTTTATACTTTTGGAGCAGC-3'. The recombinant plasmid pET-YDL124 constructed in the previous research [11] was used as a template. The PCR conditions were identical to those described above. The PCR product was cloned into pGEM-T and transformed into *E. coli* XL1-Blue. The YDL124W gene in pGEM-T vector was cut with *Nco*I and

*Hind*III and then ligated downstream of the first T7 promoter of the pACYGDH vector and used to transform *E. coli* BL21 (DE3). The recombinant plasmid was designated as pACR124-GDH.

*E. coli* cells containing one vector (pACR124-GDH) or two vectors (pETR124 plus pACGDH) were cultured at 20° C in Luria-Bertani medium (1% tryptone, 0.5% yeast extract and 0.5% NaCl) containing 100 µg/mL of ampicillin (for pETR124) and 170 µg/mL of chloramphenicol (for pACR124-GDH and pACGDH). When the cells reached an optical density (OD<sub>600 nm</sub>) of 0.5, expression was induced via the addition of 1 mM isopropyl thio-β-D-galactoside (IPTG). Cultivation was continued for an additional 24 h, after which the cells were harvested via 10 min of centrifugation at 10,000×g at 4° C and suspended in a 1/20 volume of 50 mM potassium phosphate buffer (pH 6.5).

To render the cell membrane permeable to the substrates and cofactor, the recombinant cells were mixed and shaken at 300 rpm and 30° C for 10 min with 5 mM EDTA and 1% toluene [29], washed by 10 min of centrifugation at 3,000×g, and used for the whole cell coupling reaction.

## 3. Results

### 3.1. Screening of enantioselective reductase

In a previous study, we generated 10 different microbial reductases in *E. coli* cells [11]. First, their reductase activities toward ECOB were measured via a spectrophotometric method (Table 1). Reductase activity was assayed in accordance with the basic principle that NAD(P)H was oxidized when the substrate was reduced by the enzyme. The majority of the *E. coli* cell-free extracts evidenced measurable reductase activity (0.1–6.6 U/mL) toward ECOB (Table 1). Among them, the cell-free extracts containing YDL124W, YOR120W, and YOL151W evidenced relatively high levels of activity. GC analysis was subsequently performed to detect ECHB enantiomers as the reaction products. YDL124W reductase exclusively generated (*S*)-ECHB, but YOR120W and YOL151W exclusively generated (*R*)-ECHB (Table 1).

### 3.2. Homology modeling and evaluation

To rationalize the observed enantioselectivity of YDL124W, YOR120W, and YOL151W toward ECOB, we first conducted computer modeling experiments. It has already been established that the hydride transfer from NADPH to substrate was the decisive factor in

**Table 1**  
Screening of reductase suitable for the reduction of ECOB to ECHB.

No.	GenBank locus tag	Reported/putative function	Reductase activity (U/mL)	
			ΔNAD(P)H <sup>a</sup>	ΔECHB <sup>b</sup>
<i>Saccharomyces cerevisiae</i>				
1	YJR096W	Aldo-keto reductase	0.161 (NADH)	—
2	YDL124W	Alpha-keto amide reductase	2.683 (NADPH)	0.227 ( <i>S</i> )
3	YOR120W	Glycerol dehydrogenase	1.108 (NADPH)	0.243 ( <i>R</i> )
4	YGL185C	Hydroxy acid dehydrogenase	0.106 (NADH)	—
5	YPL113C	Glyoxylate reductase	0.093 (NADH)	—
6	YDR541C	Dihydrokaempferol 4-reductase	0.062 (NADH)	—
7	YCR107W	Aryl-alcohol dehydrogenase	0.186 (NADH)	—
8	YOL151W	Methylglyoxal reductase	6.658 (NADPH)	0.194 ( <i>R</i> )
<i>Leuconostoc citreum</i>				
9	LCK_01181	Oxidoreductase	0.199 (NADH)	—
<i>Corynebacterium glutamicum</i>				
10	NCgl2041	Oxidoreductase	0.126 (NADH)	—

<sup>a</sup> Reaction mixtures contain 1 mM ECOB, 0.2 mM NAD(P)H, and 5–50 µL cell-free extract in 1 mL of 50 mM potassium phosphate (pH 6.5). Spectrophotometric assays were used.

<sup>b</sup> Reaction mixtures contain 5 mM ECOB, 1 mM NAD(P)H, 1 U crude reductase (spectrophotometer assay), 7.5 mM glucose, 2 U commercial GDH in 5 mL of 50 mM potassium phosphate (pH 6.5). The reaction products were analyzed using GC method. One unit of enzyme was defined as the amount of enzyme catalyzing the production of 1 µmol ECHB in 1 min at 30 °C.

determining the enantioselectivity of dihydrofolate reductase [30–32]. We also hypothesized that the enantioselectivity originated in the hydride transfer step, and thus we focused our computer modeling on this step.

The 3D model structure of YOL151W was reported recently by our group [11]. In this study, from a similar structure search by HHpred/HHsearch [14,15] for YDL124W and YOR120W, two X-ray crystal structures, 3BUV [12] and 1C9W [13] are obtained as potential homology templates, respectively. We superimposed the active sites of two target proteins with each of the X-ray crystal templates. 3D structural alignments for YDL124W-3BUV and YOR120W-1C9W were conducted using their entire lengths and secondary structures (supplementary data 1 and 2).

Initial structures were refined by energy minimization and MD simulations. Obviously, the total energies of the two systems remained in equilibrium after 150 ps. The average structures calculated during the entire 500 ps MD simulations were used as the final models for YDL124W and YOR120W. The RMS values for the main chains for YDL124W-3BUV and YOR120W-1C9W were calculated as 0.72 Å and 1.63 Å, respectively.

Final models of YDL124W and YOR120W were evaluated by Profile-3D [27,28] and Procheck [26]. The Profile-3D evaluations yielded compatibility scores for YDL124W and YOR120W of 202 and 199, respectively, which is close to 208, the expected score for a protein of this size. In the Procheck assessment, the reliability backbone torsion angles  $\psi$ - $\phi$  of the target proteins were examined, and the templates were evaluated for comparison. The percentages of  $\psi$ - $\phi$  angles in the core Ramachandran region were 87.1 and 86.3% for YDL124W and YOR120W, respectively, which are comparable to the template avg. 89.7%.

### 3.3. Docking of the ECOB into YDL124W, YOL151W and YOR120W

The resulting conformations of ECOB-YDL124W, ECOB-YOL151W, and ECOB-YOR120W complexes from the docking simulation using AutoDock 4.0 are shown in Fig. 1A–C, respectively. Interaction energies between each amino acid of the active site and ECOB were conducted, with the objective of evaluating the docking results in general and identifying the significant binding-site residues. The channel structures of YDL124W, YOL151W, and YOR120W for the passage of the substrates were presented in supplementary data 3.

Tyr64 and His122 were shown to cast a large shadow on ECOB bound to YDL124W. They corresponded to Tyr58 and Glu120 in 3BUV. The carbonyl oxygen connected to the methyl chloride moiety of ECOB forms hydrogen bonds with Tyr64 and His122. A hydrogen bond is also formed (avg. distance; 3.39 Å) between the second carbonyl group of ECOB and Lys30 (supplementary data 4). The latter hydrogen bond was not found in the x-ray structure of ARK1D1 complex with steroids. Thus this is one of unique features of ECOB of YDL124W. These hydrogen bonding interactions may serve to enhance the stability of the ECOB-YDL124W complex.

Ser127 and Tyr165 have been identified as the most important residues for ECOB binding into the active site of YOL151W. In YOL151W, these residues are conserved in the 1Y1P, corresponding to Ser133 and Tyr177, respectively. The carbonyl oxygen connected to the methyl chloride group of ECOB forms two hydrogen bonds with Ser127 and Tyr165. Phe87, Phe132, Met134, and Leu235 in the active site are indispensable residues, and account for the hydrophobic interactions with ECOB. The total interaction energy of ECOB with

YDL124W is slightly greater than that of YOL151W (−44.59 kcal/mol vs. −40.87 kcal/mol) arising from the more hydrogen bonds. In addition, representative plots for possible backbone torsion angles of NADPH in complex with YOL151W were presented in supplementary data 5 and 6.

In the ECOB-YOR120W complex, our docking results showed that Tyr56 (corresponding to Tyr48 in 1C9W) and His112 (His110 in 1C9W) may perform important functions in ECOB binding. Tyr56 and His112 form hydrogen bonds with carbonyl oxygen atoms at the methyl chloride end of ECOB. Total interaction energy in the complex is −42.71 kcal/mol. In addition, the aliphatic chain of Leu128 and aromatic rings of Trp113, which are located around the ethyl group of ECOB, appears to be relevant to hydrophobic interaction (supplementary data 7).

### 3.4. Purification and characterization of YDL124W

In an effort to evaluate the reaction properties of YDL124W, we purified the recombinant enzyme. Because the enzyme harbored a His tag at its C-terminal region, it could be readily purified via two sequential purification steps: Ni-NTA column and PD-10 column chromatography. The purified enzyme had a specific activity of 1.22 U/mg toward the ECOB substrate.

Its optimal reaction conditions were evaluated via the spectrophotometric method. Analysis of the initial reaction rate showed that its optimum temperature was 45 °C, and its enzyme activity was rapidly reduced at temperatures over 45 °C (Fig. 2A). It was stable up to 25 °C for 30 min, and its thermal stability was rapidly reduced over 30 °C (Fig. 2B). Its optimum pH was 6.5, and it was stable for 30 min at a pH range of 5–8 (Fig. 2C and D).

In order to convert large quantities of substrate using the reductase, the reaction process should be coupled with a GDH enzyme that regenerates NADPH. However, as these coupling reactions proceeded, a large quantity of glucose was oxidized into gluconic acid and the pH of the solution was decreased. Therefore, the selection of a buffer system is a matter of critical importance. YDL124W reductase activity was measured in an increasing molar concentration of potassium phosphate buffer (pH 6.5). Reductase activity was maintained at a constant level in a range of 50–300 mM (Fig. 2E).

On the other hand, as low substrate solubility is another problem in the enzyme reaction, the substrate was dissolved in DMSO at a concentration of 1 M and then utilized for the reaction. Reductase activity was measured with an increasing concentration of DMSO in order to elucidate the effects of DMSO (Fig. 2F). DMSO reduced enzyme activity only slightly up to a concentration of 3%, but its inhibitory effects evidenced a detectable increase at concentrations over 5%.

The kinetic parameters,  $k_{cat}$  and  $K_m$  values, for ECOB were calculated as 112 min<sup>−1</sup> and 1.08 mM, respectively (Table 2). The kinetic parameters for NADPH were 102 min<sup>−1</sup> and 4.36 μM, respectively (supplementary data 8).

### 3.5. Production of (S)-ECHB by reductase YDL124W-GDH-coupling reaction system

To maintain the ketone reduction reaction for a prolonged period, abundant NADPH must be supplied. However, as NADPH is a rather expensive material, a NADPH regeneration system is clearly required. In this study, we utilized a GDH-coupling reaction for NADPH recycling.

Reaction products from the reductase YDL124W-GDH-coupling reaction were analyzed with a GC system equipped with a chiral column. (R)-ECHB could not be detected at all, and this result implied that the enantiomeric excess was almost 100%.

As the coupling reaction continued, gluconic acid accumulated and the pH of the solution was consequently reduced. The optimum pH of YDL124W reductase was pH 6.5, and its activity rapidly decreased

**Table 2**  
Kinetic parameters of YDL124W.

	$k_{cat}$ (min <sup>−1</sup> )	$K_m$ (mM)	$k_{cat}/K_m$ (min <sup>−1</sup> mM <sup>−1</sup> )
ECOB	112	1.08	104
NADPH	102	0.00436	23400

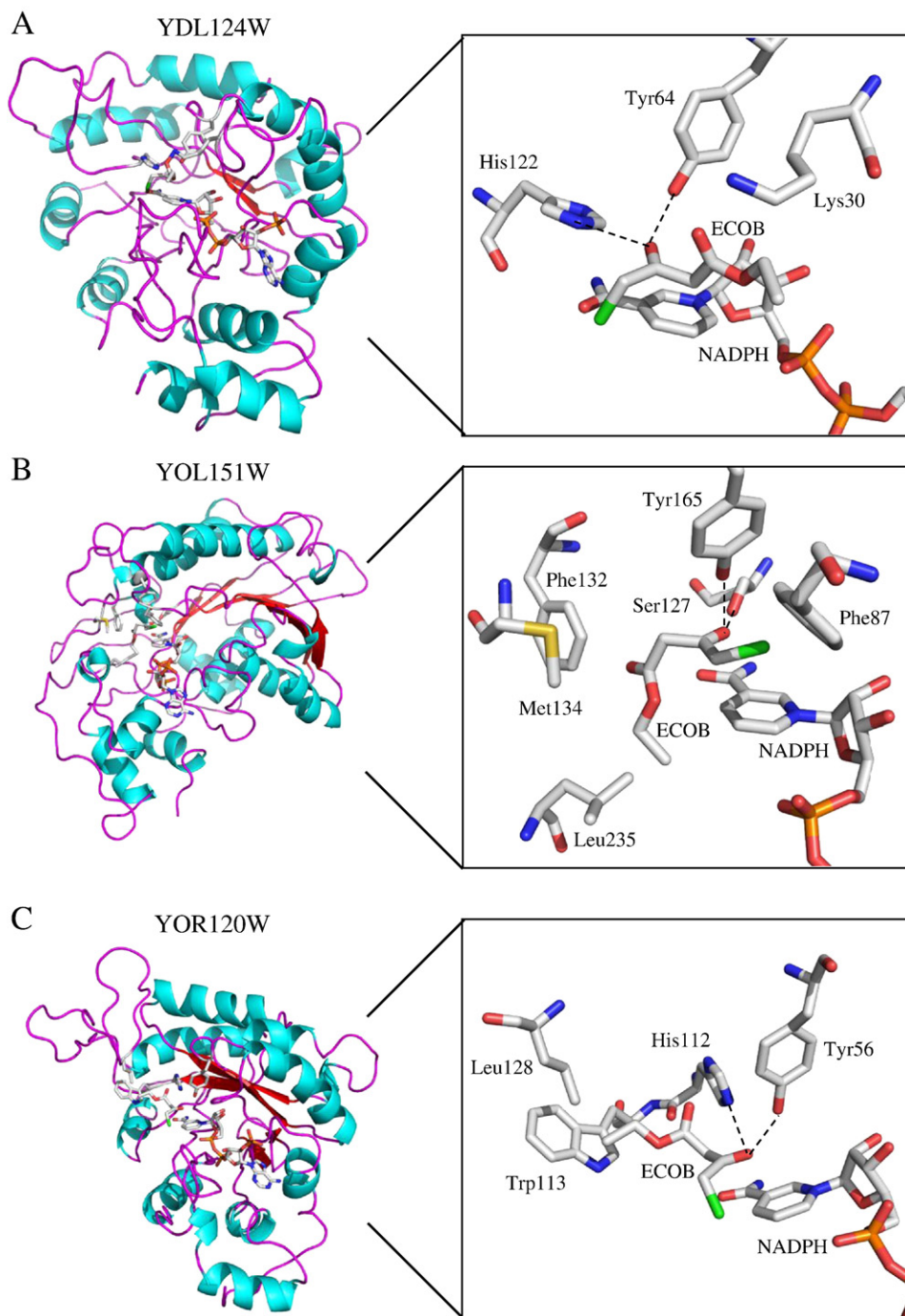


**Fig. 1.** Homology models and docking models. Homology models of YDL124W and YOR120W were constructed based on the crystal structures of 3BUV and 1C9W, respectively. The homology model of YOL151W was cited [11]. ECOB and NADPH were docked into the enzyme active sites of YDL124W (A), YOL151W (B), and YOR120W (C), respectively. The coloring scheme shows nitrogen atoms in blue, oxygen atoms in red, carbon atoms in light grey, sulfur atom in yellow, phosphorus atoms in orange, and chlorine atoms in green. Dotted lines indicate the expected hydrogen bonds.

below pH 6.0. In this experiment, the pH of the solution was maintained within pH 6.0–6.5 via occasional additions of 1 M NaOH solution.

When the coupling reaction was conducted with initial substrate concentrations of 100 mM, approximately 70% of the ECOB was converted to (*S*)-ECHB with enantiomeric excess of 96% within 240 min (Fig. 3).

### 3.6. Coupling reaction using an *E. coli* whole cell system

We used the pETR124 plasmid [11] for the production of the reductase enzyme. Additionally, we constructed two recombinant

plasmids in this research. The pACGDH plasmid contained the *B. subtilis* GDH gene (GenBank ID EF626962.1) and the pACR124-GDH plasmid harbored both the GDH gene and the reductase gene (Fig. 4A). The results of SDS-PAGE analysis revealed that *E. coli* cells containing both pETR124 and pACGDH generated both reductase and GDH (Fig. 4B) and *E. coli* cells containing only pACR124-GDH also generated these two enzymes (Fig. 4B).

The reductase and GDH activities of four different recombinant *E. coli* cells were measured using a whole cell system (Table 3). As anticipated, *E. coli* intact cells containing pETR124 or pACGDH evidenced either reductase or GDH activities exclusively. *E. coli* cells

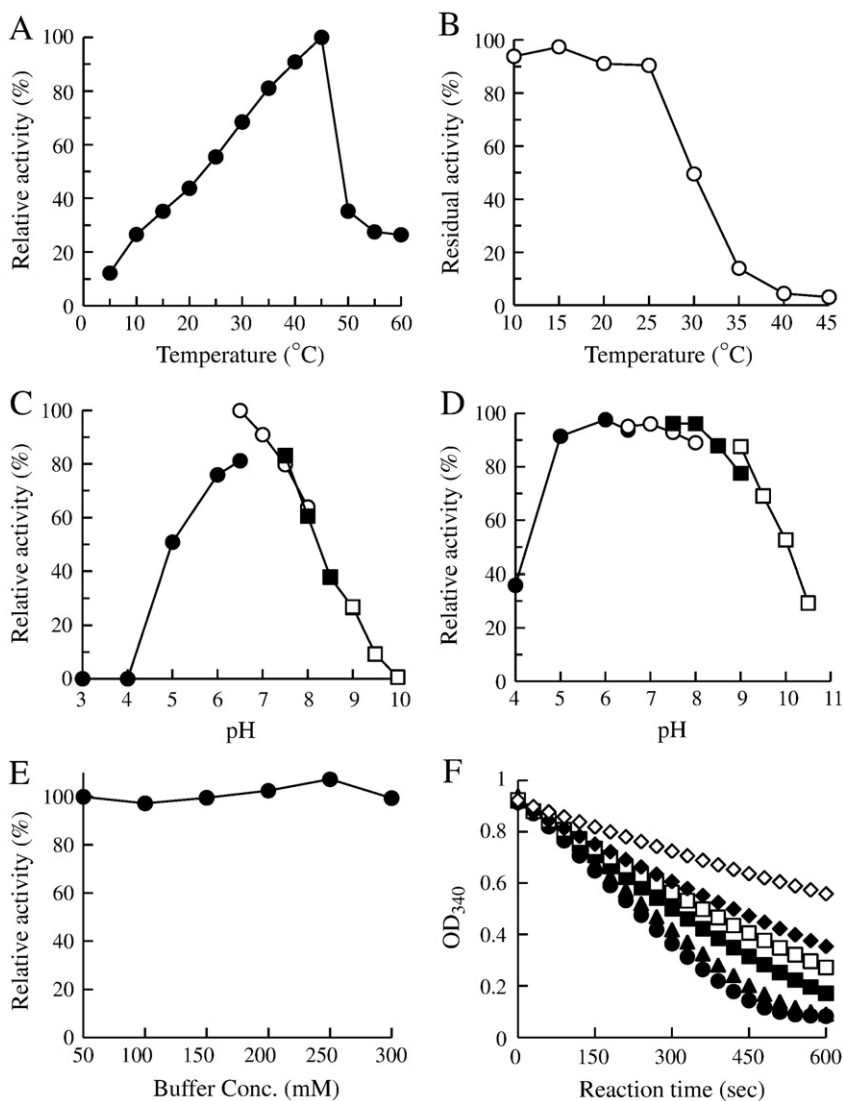


**Fig. 2.** Reaction properties of YDL124W reductase. Reductase activity was determined by measurements of the reduction in NADPH absorption at 340 nm. (A) Reductase activity was measured at various temperatures. (B) After 30 min of pre-incubation at various temperatures, residual reductase activity was measured at 30 °C. (C) Reductase activity was measured at various pHs using buffers including acetic acid/sodium acetate (●), potassium phosphate (○), Tris-HCl (■), and glycine-KCl-KOH buffers (□). (D) After 30 min of pre-incubation at various pHs, residual reductase activity was measured at pH 6.5. (E) The effect of potassium phosphate buffer concentration was determined. (F) The effects of DMSO concentration were determined. 1% (●), 3% (▲), 10% (■), 15% (□), 20% (◆), 30% (◇).

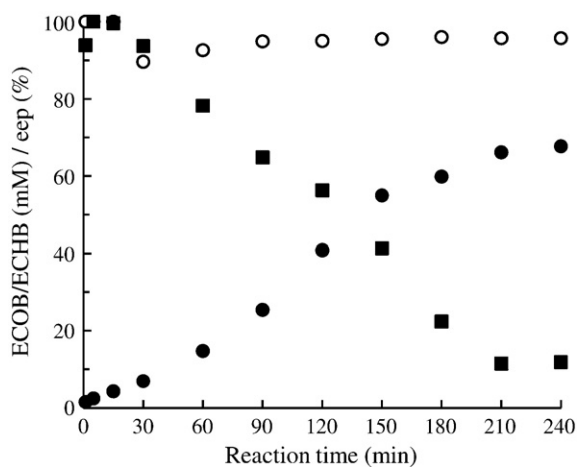


**Fig. 3.** (S)-ECHB production via the reductase-GDH-coupling reaction. The amounts of ECOB (■), (S)-ECHB (●), and enantiomeric excess values (○) were measured over the time course.

harboring two plasmids (pETR124 and pACGDH) evidenced both reductase and GDH activities simultaneously. Additionally, *E. coli* cells containing pACR124-GDH exhibited both activities, although the GDH activity was substantially higher than the reductase activity.

We conducted whole cell coupling reactions using the latter two *E. coli* cell systems. The coupling reactions worked well in these *E. coli* whole cell systems (Fig. 5). Using a 100 mM initial concentration of the ECOB substrate, the conversion yield reached a level of 80% within 180 min. (S)-ECHB was exclusively produced with an enantiomeric excess value of 98% in both reaction systems.

#### 4. Discussion

(S)-ECHB is a chiral intermediate of many hyperlipidemia drugs including Atorvastatin, as mentioned above. This compound could be generated from ECOB, a prochiral ketone compound, via the process of enantioselective reduction. For the efficient production of (S)-ECHB, therefore, a suitable reductase enzyme should be employed. In this study, YDL124W, YOL151W, and YOR120W reductases were selected for the production of chiral ECHB among 10 different microbial

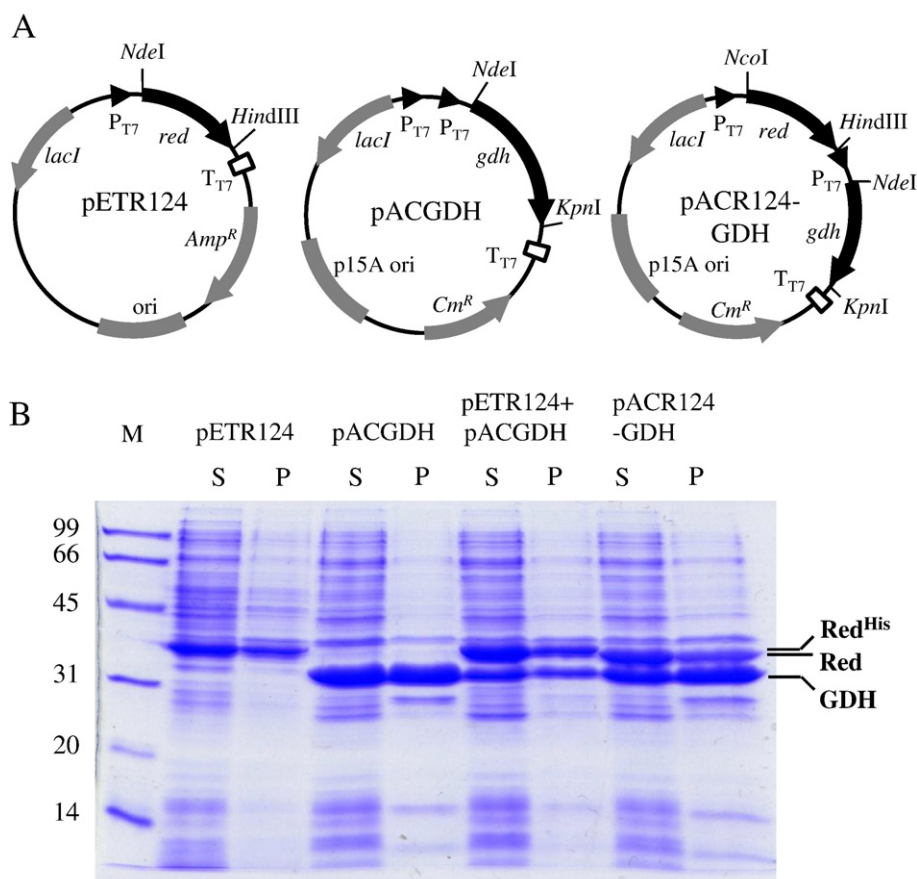


**Fig. 4.** Recombinant plasmid construction and SDS-PAGE. (A) Three recombinant plasmids, pETR124 (YDL124W), pACGDH (*Bacillus* GDH), and pACR124-GDH (YDL124W and GDH), were constructed. (B) SDS-analysis was conducted for four different recombinant *E. coli* cells containing pETR124, pACGDH, pETR124 plus pACGDH, and pACR124-GDH, respectively. Red<sup>His</sup> means reductase with His tag. S and P mean supernatant and precipitate after cell lysis via sonication.

reductases. These three enzymes have been reported in several previous reports, and their substrate specificity and enantioselectivity toward a variety of compounds have also been characterized. We confirmed that YDL124W generated (*S*)-ECHB exclusively, whereas YOR120W and YOL151W exclusively generated (*R*)-ECHB.

In this study, in an effort to compare and explain their enantioselective reaction mechanisms at the molecular level, we conducted homology modeling and docking modeling. Interestingly, three binding models may be comparable with the substrate binding crystal structures of 3BUV (corresponding to YDL124W), 1Y1P (YOL151W) and 1C9W (YOR120W), respectively [9,12,13]. These similarities imply the reliability of our docking results. The results indicated that three complexes were similar with regard to their hydrophilic interactions, but evidenced different enantioselectivity characteristics due to hydrophobic interactions with surrounding residues.

Among three enzymes, we focused on YDL124W reductase because it exclusively generated the (*S*)-form product. 3D structure alignment of binding pocket of AKR1D1–steroid complex with YDL124W model structure containing bound ECOB is shown Fig. 6.  $\Delta^4$ -3-ketosteroids are substrates for mammalian steroid carbon-carbon double bond reductase (ARK1D1), where they mainly undergo

to catalyze reduction of  $\Delta^4$ -ene double bonds through the 4-pro-*R* hydride transferred from the *re*-face of the nicotinamide ring of the NADPH cofactor to C5 of the steroid substrate. In contrast, the substrate in the YDL124W-ECOB complex by automatic AutoDock docking procedure adopts different anti-conformation as not observed in AKR1D1–steroid complex structure, indicating a different orientation of the ECOB in the YDL124W. This observation appears to result from the introduction of the steric bulk of the His120 (YDL124W)

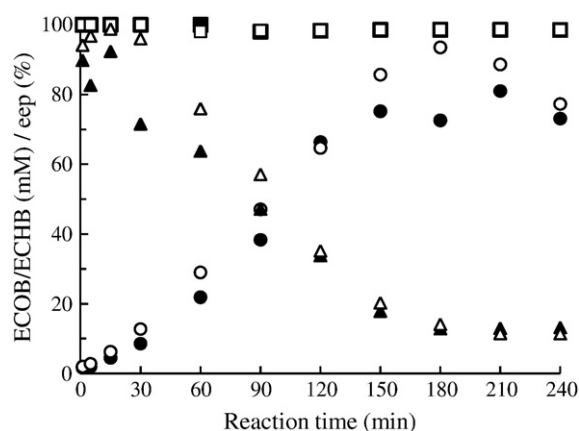


**Fig. 5.** Production of (*S*)-ECHB by whole cell coupling reaction. The conversion yield and e.e. values were measured over the time course. ECOB (▲) and (*S*)-ECHB (●) via the one plasmid (pACR124-GDH) were measured. ECOB (△) and (*S*)-ECHB (○) via two-plasmid systems (pETR124 plus pACGDH) were also measured. Enantiomeric excess values by the one-plasmid (■) and two-plasmid systems (□) were measured.

**Table 3**  
Enzyme activity of recombinant *E. coli* whole cells.

Plasmid	Reductase activity (U/mL)	GDH activity (U/mL)
pETR124	1.95	N.D.
pACGDH	N.D.	9.66
pETR124 + pACGDH	3.35	3.80
pACR124GDH	1.66	5.29

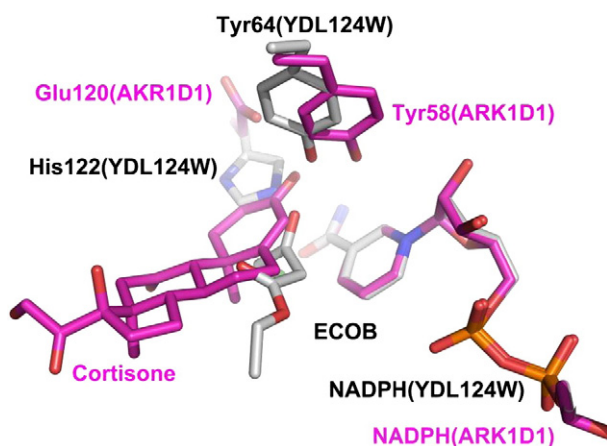


**Fig. 6.** 3D structure alignment of binding pocket of AKR1D1-steroid complex with YDL124W model structure containing bound ECOB, NADPH, cortisone, Tyr58, and Glu120 in the active site of AKR1D1 (magenta color) were compared with NADPH, ECOB, Tyr64, and His122 in the active site of YDL124W (same colors used in Fig. 1).

imidazole side chain by the replacement of its corresponding Glu120 residue in AKR1D1. As a result, the 4-pro-(*R*)-hydride of the NADPH cofactor would be adjacent to the ECOB carbonyl group (to C-5 of the substrate carbon-carbon double bond in the AKR1D1) in the YDL124W active site.

The simulations of ECOB bound to the YDL124W were started from catalytically active pose with the carbonyl group with methyl chloride of ECOB being positioned close to and oriented toward the nicotinamide ring of the cofactor in all MD simulations. In the simulations of the YDL124W-ECOB complex, the 4-pro-(*R*)-hydride of

NADPH cofactor turned upwards shown in Fig. 6, with the carbonyl group pointing toward the nicotinamide, forming the orientation for a possible hydride transfer.

YDL124W has already been purified from *S. cerevisiae*, and its properties have been characterized [33]. YDL124W has been identified as an NADPH-dependent alpha-keto amide reductase that exhibits reducing activity not only for aromatic alpha-keto amides, but also for aliphatic and aromatic alpha-keto esters. Although the substrate specificity and stereoselectivity of the enzyme have previously been reported in the literature, no 3D-structural studies have yet been conducted. Therefore, an explanation of the reaction mechanism using the active site-substrate docking model is clearly meaningful.

As shown in our docking model of YDL124W (Figs. 1A and 7A), the carbonyl oxygen atom of ECOB, which is located close to the nicotinamide ring, forms hydrogen bonds with Tyr64 and His122. The C4 atom of the nicotinamide ring may possibly donate its hydrogen atom to the carbonyl carbon atom of the ECOB, with a distance of 3.1 Å between the C4 atom and the carbonyl carbon. The proposed catalytic mechanism is as follows. The carbonyl oxygen atom of the substrate forms hydrogen bonds with both the Tyr and His residues, and is protonated from the Tyr residue, followed by the attack of a hydrogen atom from the C4 atom of NADPH against the carbonyl carbon atom of the substrate. Meanwhile, the nicotinamide mononucleotide (NMN) ring of the cofactor is located at the *re*-face of ECOB. Thus, this ketone should be reduced to (*S*)-ECHB, which is consistent with our experimental observations (Fig. 3). On the other hand, in the cases of YOR120W and YOL151W, the NMN ring of the cofactor appeared to be located at the *si*-face of ECOB. Thus, this ketone should be reduced to (*R*)-ECHB (Fig. 7B).

Recently, some reductase reactions have been conducted using whole cell systems. In the current study, we co-expressed both reductase and *Bacillus* glucose dehydrogenase in the same *E. coli* cell, using one-vector and two-vector systems. The two enzymes were successfully expressed in the *E. coli* cells and NADPH recycling was

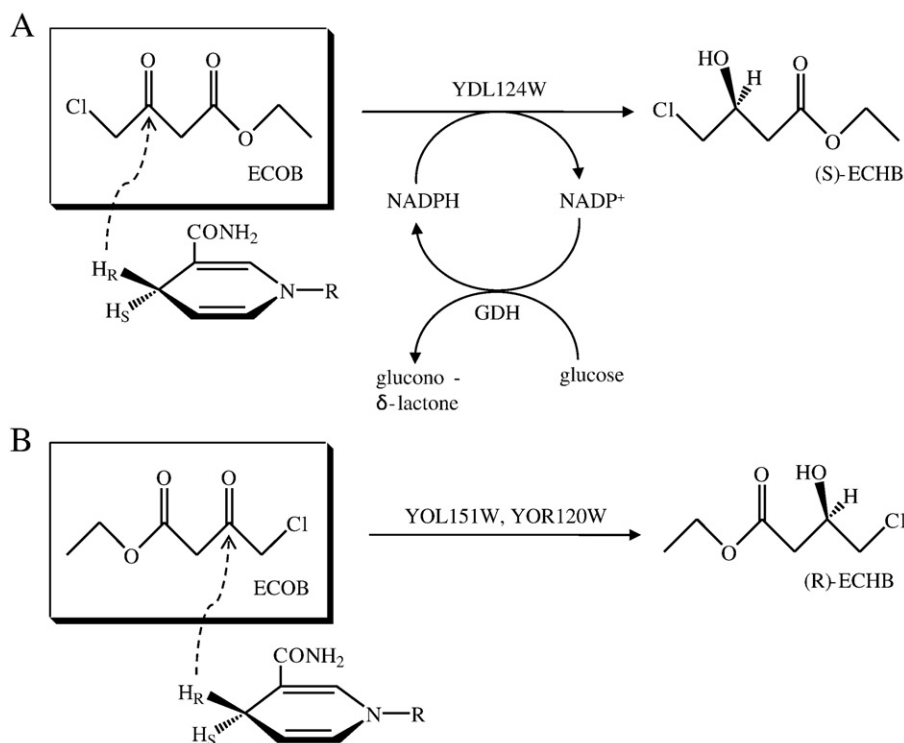


**Fig. 7.** Stereochemistry of reductase and schematic representation of the reduction process. (A) YDL124W converted ECOB into (*S*)-ECHB. (B) YOL151W and YOR120W converted ECOB into (*R*)-ECHB.

conducted. Using this *E. coli* whole cell system, we were able to effect the conversion of ECOB into (S)-ECHB.

Collectively, we proposed the detailed mechanism whereby YDL124W produced (S)-ECHB exclusively, and demonstrated that this enzyme could generate (S)-ECHB together with a glucose dehydrogenase-coupling reaction. Additionally, by adopting the whole cell system, this coupling system might prove able to generate high concentrations of (S)-ECHB.

## 5. Conclusions

Baker's yeast YDL124W, YOR120W, and YOL151W reductases showed high activities for ECOB. YDL124W produced (S)-ECHB exclusively, whereas YOR120W and YOL151W made (R)-form alcohol. Homology models and docking models with ECOB and NADPH elucidated their substrate specificity and enantioselectivity; in the case of YDL124W, the nicotinamide mononucleotide (NMN) ring of the cofactor is located at the *re*-face of ECOB, whereas in the case of YOR120W and YOL151W, the NMN ring of the cofactor is located at the *si*-face of ECOB. Recombinant *E. coli* cells co-expressing YDL124W and *B. subtilis* glucose dehydrogenase could recycle NADPH and convert ECOB into (S)-ECHB continuously.

## Acknowledgement

This work was supported by the 21C Frontier Microbial Genomics and Applications Center Program, Ministry of Education, Science & Technology, Republic of Korea, and Gyeonggi Regional Research Center (GRRCC) at the Catholic University of Korea.

## Appendix A. Supplementary data

Supplementary data associated with this article can be found, in the online version, at doi:10.1016/j.bbapap.2010.06.011.

## References

- [1] K. Goldberg, K. Schroer, S. Lütz, A. Liese, Biocatalytic ketone reduction—a powerful tool for the production of chiral alcohols—part I: processes with isolated enzymes, *Appl. Microbiol. Biotechnol.* 76 (2007) 237–248.
- [2] K. Schroer, U. Mackfeld, I.A.W. Tan, C. Wandrey, F. Heuser, S. Bringer-Mayer, A. Weckbecker, W. Hummel, T. Daußmann, R. Pfäler, A. Liese, S. Lütz, Continuous asymmetric ketone reduction processes with recombinant *Escherichia coli*, *J. Biotechnol.* 132 (2007) 438–444.
- [3] K. Inoue, Y. Makino, N. Itoh, Production of (R)-chiral alcohols by a hydrogen-transfer bioreduction with NADH-dependent *Leifsonia* alcohol dehydrogenase (LSADH), *Tetrahedron: asymmetry* 16 (2005) 2539–2549.
- [4] I.A. Kaluzna, B.D. Feske, W. Wittayanan, I. Ghiviriga, J.D. Stewart, Stereoselective, biocatalytic reductions of  $\alpha$ -chloro- $\beta$ -keto esters, *J. Org. Chem.* 70 (2005) 342–345.
- [5] T. Ema, H. Yagasaki, N. Okita, M. Takeda, T. Sakai, Asymmetric reduction of ketones using recombinant *E. coli* cells that produce a versatile carbonyl reductase with high enantioselectivity and broad substrate specificity, *Tetrahedron* 62 (2006) 6143–6149.
- [6] J.C. Moore, D.J. Pollard, B. Kosjek, P.N. Devine, Advances in the enzymatic reduction of ketones, *Acc. Chem. Res.* 40 (2007) 1412–1419.
- [7] Z. Xu, Y. Liu, L. Fang, X. Jiang, K. Jing, P. Cen, Construction of a two-strain system for asymmetric reduction of ethyl 4-chloro-3-oxobutanoate to (S)-4-chloro-3-hydroxybutanoate ethyl ester, *Appl. Microbiol. Biotechnol.* 70 (2006) 40–46.
- [8] M. Ernst, B. Kaup, M. Muller, S. Bringer-Meyer, H. Sahm, Enantioselective reduction of carbonyl compounds by whole-cell biotransformation, combining a formate dehydrogenase and a (R)-specific alcohol dehydrogenase, *Appl. Microbiol. Biotechnol.* 66 (2005) 629–634.
- [9] S. Kamitori, A. Iguchi, A. Ohtaki, M. Yamada, K. Kita, X-ray structures of NADPH-dependent carbonyl reductase from *Sporobolomyces salmonicolor* provide insights into stereoselective reductions of carbonyl compounds, *J. Mol. Biol.* 352 (2005) 551–558.
- [10] T.R. Cundari, A. Dinescu, D. Zhu, L. Hua, A molecular modeling study on the enantioselectivity of aryl alkyl ketone reductions by a NADPH-dependent carbonyl reductase, *J. Mol. Model.* 13 (2007) 685–690.
- [11] H.C. Yun, H.J. Choi, D. Kim, K.N. Uhm, H.K. Kim, Asymmetric synthesis of (S)-3-chloro-1-phenyl-1-propanol using *Saccharomyces cerevisiae* reductase with high enantioselectivity, *Appl. Microbiol. Biotechnol.* 87 (2010) 185–193.
- [12] L. Di Costanzo, J.E. Drury, T.M. Penning, D.W. Christianson, Crystal structure of human liver Delta4-3-ketosteroid 5beta-reductase (AKR1D1) and implications for substrate binding and catalysis, *J. Biol. Chem.* 283 (2008) 16830–16839.
- [13] Q. Ye, D. Hyndman, X. Li, T.G. Flynn, Z. Jia, Crystal structure of CHO reductase, a member of the aldo-keto reductase superfamily, *Proteins* 38 (2000) 41–48.
- [14] J. Söding, Protein homology detection by HMM-HMM comparison, *Bioinformatics* 21 (2005) 951–960.
- [15] J. Söding, A. Biegert, A.N. Lupas, The HHpred interactive server for protein homology detection and structure prediction, *Nucleic Acids Res.* 33 (2005) W244–W248.
- [16] A. Sali, T.L. Blundell, Comparative protein modeling by satisfaction of spatial restraints, *J. Mol. Biol.* 234 (1993) 779–815.
- [17] J. Schymkowitz, J. Borg, F. Stricher, R. Nys, F. Rousseau, L. Serrano, The FoldX web server: an online force field, *Nucleic Acids Res.* 33 (2005) W382–W388.
- [18] D.A. Pearlman, D.A. Case, J.W. Caldwell, W.S. Ross, T.E. Cheatham, S. Debolt, D. Ferguson, G. Seibel, P. Kollman, Amber, a package of computer-programs for applying molecular mechanics, normal-mode analysis, molecular-dynamics and free-energy calculations to simulate the structural and energetic properties of molecules, *Comput. Phys. Commun.* 91 (1995) 1–41.
- [19] D.A. Case, T.E. Cheatham, T. Darden, H. Gohlke, R. Luo, K.M. Merz, A. Onufriev, C. Simmerling, B. Wang, R.J. Woods, The Amber biomolecular simulation programs, *J. Comput. Chem.* 26 (2005) 1668–1688.
- [20] R. Huey, G.M. Morris, A.J. Olson, D.S. Goodsell, A semiempirical free energy force field with charge-based desolvation, *J. Comput. Chem.* 28 (2007) 1145–1152.
- [21] Y. Duan, C. Wu, S. Chowdhury, M.C. Lee, G.M. Xiong, W. Zhang, R. Yang, P. Cieplak, R. Luo, T. Lee, J. Caldwell, J.M. Wang, P.A. Kollman, point-charge force field for molecular mechanics simulations of proteins based on condensed-phase quantum mechanical calculations, *J. Comput. Chem.* 24 (2003) 1999–2012.
- [22] J. Wang, R.M. Wolf, J.W. Caldwell, P.A. Kollman, D.A. Case, Development and testing of a general amber force field, *J. Comput. Chem.* 25 (2004) 1157–1174.
- [23] B. Huang, M. Schroeder, Using protein binding site prediction to improve protein docking, *Gene* 422 (2008) 14–21.
- [24] A. Fisher, R.K.G. Do, A. Sali, Modeling of loops in protein structures, *Protein Sci.* 9 (2000) 1–21.
- [25] M.Y. Shen, A. Sali, Statistical potential for assessment and prediction of protein structures, *Protein Sci.* 15 (2006) 2507–2524.
- [26] R.A. Laskowski, M.W. MacArthur, D.S. Moss, J.M. Thornton, PROCHECK: a program to check the stereochemical quality of protein structures, *J. Appl. Cryst.* 26 (1993) 283–291.
- [27] R. Luthy, U.J. Bowie, D. Eisenberg, Assessment of protein models with three dimensional profiles, *Nature* 356 (1992) 83–85.
- [28] Profile-3D User Guide, Accelrys Inc, San Diego, 1999.
- [29] W. Zhang, K. O'Connor, D.I.C. Wang, Z. Li, Bioreduction with efficient recycling of NADPH by coupled permeabilized microorganisms, *Appl. Environ. Microbiol.* 75 (2009) 687–694.
- [30] M. Garcia-Viloca, D.G. Truhlar, J. Gao, Reaction-path energetics and kinetics of the hydride transfer reaction catalyzed by dihydrofolate reductase, *Biochemistry* 42 (2003) 13558–13575.
- [31] W. Nowak, V. Cody, A. Wojtczak, Computer modeling studies of the structural role of NADPH binding to active site mutants of human dihydrofolate reductase in complex with piritrexim, *Acta Biochim. Pol.* 48 (2001) 903–916.
- [32] P.L. Cummins, J.E. Gready, Molecular dynamics and free energy perturbation study of hydride-ion transfer step in dihydrofolate reductase using combined quantum and molecular mechanical model, *J. Comp. Chem.* 19 (1998) 977–988.
- [33] K. Ishihara, H. Yamamoto, K. Mitsuhashi, K. Nishikawa, S. Tsuboi, H. Tsuji, N. Nakajima, Purification and characterization of alpha-keto amide reductase from *Saccharomyces cerevisiae*, *Biosci. Biotechnol. Biochem.* 68 (2004) 2306–2312.